Boundary-Layer Transition on a Cone and Flat Plate at Mach 3.5

F.-J. Chen* and M. R. Malik†
High Technology Corporation, Hampton, Virginia
and
I. E. Beckwith‡
NASA Langley Research Center, Hampton, Virginia

Boundary-layer transition data on a cone and flat plate obtained in the Mach 3.5 Pilot Low-Disturbance Tunnel at NASA Langley are presented. Measured flat-plate transition Reynolds numbers in this tunnel are an order of magnitude higher than previous results obtained in conventional noisy supersonic wind tunnels. Transition predictions based on compressible linear stability theory and the e^N method with $N=10$ are in excellent agreement with the measured locations of transition onset for both the cone and flat plate under low-noise conditions in this tunnel. This investigation has resolved the discrepancies between the results of linear stability theory and the data from conventional supersonic wind tunnels regarding the ratio of cone-to-flat-plate transition Reynolds numbers.

Nomenclature

b	= flat-plate leading-edge bluntness
F	= dimensionless frequency, $2\pi f\nu_e/u_e^2$
f	= frequency
M	= Mach number
N	= exponential factor in amplification ratio e^N from linear stability theory
P	= pressure
Pr	= Prandtl number
R	= reference Reynolds number, $(u_e s/\nu_e)^{1/2}$
R_∞	= freestream unit Reynolds number, $\rho_\infty u_\infty/\mu_\infty$
Re	= local unit Reynolds number, $\rho_e u_e/\mu_e$
Re_T	= local transition Reynolds number based on flow distance to transition
r	= recovery factor defined by $(T_{aw}-T_e)/(T_o-T_e)$
rms	= root mean square
s	= surface distance from cone tip or leading edge of flap plate
T	= temperature
u	= streamwise velocity
X	= axial distance from nozzle throat or from cone tip
$\Delta X,\Delta Y,\Delta Z$	= axial, vertical, and horizontal dimensions of quiet test core (see Fig. 1)
β	= Mach angle
μ	= dynamic viscosity
ν	= kinematic viscosity, μ/ρ
ρ	= mass density
σ	= spatial amplification rate

Subscripts

aw	= adiabatic wall
e	= local values at boundary-layer edge
L	= laminar
o	= stagnation; also onset of instability
p	= surface pitot tube
s	= cone tip or flat-plate leading edge
T	= transition onset
Tu	= turbulent
t	= pitot
w	= wall
∞	= freestream

Superscripts

$(\tilde{\ })$	= root mean square
$(\bar{\ })$	= mean value

Presented as Paper 88-0411 at the AIAA 26th Aerospace Sciences Meeting, Reno, NV, Jan. 11-14, 1988; received Feb. 4, 1988; revision received June 24, 1988.

*Senior Engineer. Member AIAA.
†President. Senior Member AIAA.
‡Leader, High Speed Boundary Layer, Stability and Transition Group, Viscous Flow Branch, Fluid Mechanics Division. Associate Fellow AIAA.

Introduction

AFTER more than 30 years of experimental and theoretical investigations related to differences between cone and flat-plate transition (see Refs. 1-3, for example), some uncertainties are still to be found. Almost two decades ago, Pate[4] concluded that valid comparisons between cone and flat-plate transition were possible only if the data were obtained in the same test facility under identical test conditions and by using equivalent methods of transition detection. Pate's correlations for end-of-transition data from five test facilities showed that the ratio of cone-to-flat-plate transition Reynolds numbers decreased from about 2.5 at Mach 3 to about 1 at Mach 8. The data[4] also indicated that for a given Mach number in the range of 3-5, this ratio tended to decrease with increasing tunnel size. This effect may have been caused by reductions in the test section noise levels with increasing tunnel size that have been measured.[5-7] These early results can therefore be taken as a hint of different responses (or receptivities) to tunnel noise by the cone and flat-plate boundary layers. That is, if the tunnel noise could be reduced further, would the cone-to-flat-plate transition Reynolds number ratios also be reduced further to 1 or less? Linear stability calculations using the e^N method would suggest that to be the case.[8,9] It has been shown[9-17] that when all input disturbances are small and when the dominant physical effects are properly accounted for in the stability equations, the e^N method provides reliable predictions of transition when N is in the range of 9-11.

The development and successful operation at NASA Langley of the Mach 3.5 Pilot Low-Disturbance Tunnel[18,19] offered the opportunity to provide some answers to the above-noted uncertainties on cone and flat-plate transition. This new facility provides stream disturbance levels that can be extremely low in the upstream part of the test rhombus. The previously dominant facility disturbances now can be essentially eliminated in the upstream sensitive regions of the cone and

flat-plate boundary layers. Since the noise levels and onset locations can be varied inside the test rhombus of this tunnel,[18] opportunities are also available to start experimental investigations into the possible different receptivities of the cone and flat-plate boundary layers. However, this paper will be limited to the consideration of the new experimental and theoretical results for transition at Mach 3.5.

The effects of leading-edge bluntness on flat-plate boundary-layer transition at supersonic speeds have been investigated previously.[6,20-23] The bluntness effects impact the heat-transfer problems on high-speed flight vehicles. Moeckel[21] showed that the delay of boundary-layer transition on blunted plates was caused by the reduction of the boundary-layer edge unit Reynolds number due to blunting. However, Reshotko and Khan[22] pointed out that Moeckel's hypothesis could not explain the systematic displacement of the transition location and its reversal behavior that were observed in wind-tunnel tests.[23-25] In order to properly characterize the progressive swallowing of streamlines in the entropy layer by the developing boundary layer, Reshotko and Kahn[22] adopted the method of multiple scales to analyze the inner- and outer-layer flows on an insulated blunt plate and found some stabilizing and destabilizing effects on the first- and second-mode disturbances due to streamline swallowing. Besides the complexity of the streamline swallowing process, Pate's data[7] indicated that the increase of transition Reynolds numbers due to increased blunting could be augmented by increases in Mach or unit Reynolds numbers. This observation suggests that the wind-tunnel noise has a predominant influence over the leading-edge bluntness effects on boundary-layer transition. The effects of a limited range of small leading-edge bluntness values on flat-plate transition are included in this investigation for the unique conditions of variable freestream noise levels in the Mach 3.5 Pilot Low-Disturbance Tunnel.

Experimental Conditions

Facility

Wind Tunnel

The Mach 3.5 Pilot Low-Disturbance Tunnel is located in the Gas Dynamics Laboratory at the NASA Langley Research Center. It is a blowdown wind tunnel that uses the large-capacity, high-pressure air and vacuum systems in the laboratory. The air is dried to a dewpoint temperature of $-47°C$ and is then reduced in pressure by control valves located some distance upstream of the settling chamber. Before entering the settling chamber, the supply air passes through a filter[26] that has nominal and absolute removal ratings of 0.4 and 1 μ, respectively.

Settling Chamber

The settling chamber is approximately 6.5 m long by 0.6 m inside diameter; it contains a honeycomb, seven turbulence screens, and several dense porous plates that function as acoustic baffles to attenuate the high-level noise (rms pressure) caused by the control valves and piping system from about 0.2% of stagnation pressure down to about 0.01%. More details on the facility including the settling chamber and the 1 μ air filter are given in Refs. 19, 26, and 27.

Nozzle

Configuration

A sketch of the nozzle wall cross sections in vertical and horizontal center planes is shown in Fig. 1. Details of the nozzle geometry and dimensions are given in a previous report.[18] The boundary-layer bleed slots located upstream of the throat on both the contour and side walls also are shown in Fig. 1. The boundary-layer bleed flow can be cut off by closing a valve downstream of the bleed plenum. Thus, with this bleed valve closed, the boundary layer in the subsonic approach

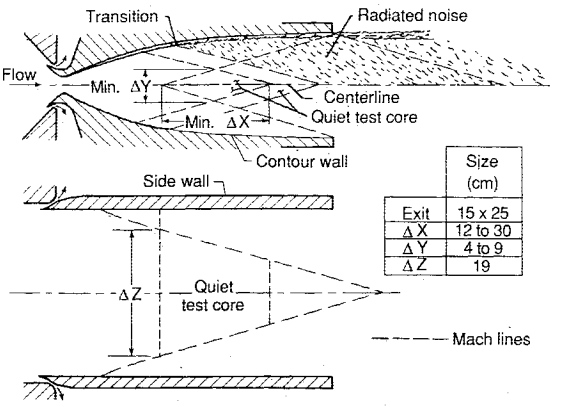

Fig. 1 Mach 3.5 two-dimensional nozzle and quiet test core in the Pilot Low-Disturbance Tunnel.

spills around the slot leading edges and the nozzle wall boundary layers are completely turbulent except at the lowest values of R_∞. With the bleed valve open, the entire boundary layers on both the contour and side walls of the subsonic approach are removed. The wall boundary layers on the upstream regions of the supersonic nozzle are then laminar and the optimum low-noise conditions in the test rhombus are obtained when the contour walls are very clean and highly polished. Due to increasing problems in maintaining the surface finish on the original contour-wall blocks, a new set of blocks were fabricated and polished. The current surface finish on the new blocks has maximum peak-to-valley roughness defects in the throat regions of about 0.5 μ. A discussion on the problems of surface finish and nozzle noise is given in Ref. 28. During the present investigation, the new nozzle blocks were installed in the tunnel.

Quiet Test Core

The dominant source of test section disturbances in conventional supersonic/hypersonic tunnels is the acoustic radiation from eddies in the turbulent boundary layers on the nozzle walls.[4-6] In supersonic flow, this noise is in the form of finite-strength wavelets that are propagated along Mach lines. Hence, as illustrated in Fig. 1, the location of transition onset in the wall boundary layers can be sensed with a hot-wire probe at any point along a Mach line extended downstream from that location, which is then the "acoustic origin" for the onset of radiated noise in the nozzle flowfield. As the unit Reynolds number is increased, the transition moves upstream along the contoured walls in this nozzle. The quiet test core region then becomes smaller and tends to approach some minimum size of streamwise length ΔX and height ΔY. When the nozzle walls are very clean and highly polished, the minimum value of ΔX is about 12 cm. At high Reynolds numbers, the sidewall boundary layers are generally turbulent. For these conditions, radiation from the side walls is minimized by the large width of the nozzle (see lower part of Fig. 1) and the small local Mach numbers ($M_e < 2.5$) at the upstream acoustic origin locations. The large width of the quiet test core ΔZ allows the testing of swept wings and models at large angle of attack.

Effect of Unit Reynolds Number on Noise in Pilot Nozzle

The rms static pressures (normalized by the mean pressures) obtained from hot-wire data on the nozzle centerline are plotted vs distance from the nozzle throat in Fig. 2. Since acoustic noise is propagated along Mach lines in supersonic flow, the noise levels in the test rhombus are extremely low (within the instrument noise range) when the boundary layers at the upstream acoustic origin regions are laminar. From the acoustic origin location at transition on the nozzle wall, the corresponding locus of the increased noise levels can be traced

along a Mach line downstream of the centerline. When the probe is traversed through this centerline station, the increased noise is sensed by the hot-wire anemometer.

Fig. 2a illustrates how the values of ΔX varied with R_∞ during the present tests with the bleed valve open. These values of ΔX were consistent and repeatable as verified from hot-wire surveys made before, during, and after the present transition data were obtained. The tip of the cone or the leading edge of the flat plate was located at either $X_s = 12.7$ or 20.3 cm during these tests. The values of ΔX listed in the figure are measured from $X = 12.7$ cm (the upstream tip of the uniform flow test rhombus[18]) to the location where a line faired through the rms data crosses the $\tilde{P}_\infty/\bar{P}_\infty = 0.1\%$ line that is used as a nominal definition of transition at the nozzle wall acoustic origins. These values of ΔX are greater than those reported[18,19,26] previously and are also obtained at higher unit Reynolds numbers due to the improved surface finish of the present nozzle blocks and the improved surface cleaning technique used.

Since, at a given unit Reynolds number, the upstream boundary of the increasing noise region is fixed within the nozzle flowfield, the noise level and onset locations on the test model can be varied, as desired, by simply moving the test model downstream within the uniform test flow rhombus. Obviously, the noise onset regions and levels can also be varied by changing the unit Reynolds number.

Another technique that has been used extensively to increase the noise levels[18] is to cut off the subsonic boundary-layer removal flow by closing the bleed valve. The bleed valve closed data shown in Fig. 2b indicates that the boundary layer on the nozzle walls then is completely turbulent except when $R_\infty/m < 1.1 \times 10^7$.

Models and Transition Detection Techniques

Two 5 deg half-angle cone models were tested previously[18,26] in this tunnel with the original nozzle blocks. Both models were fabricated of stainless steel and were 38.1 cm long. Two rows of thermocouples were installed in the 0.076 cm thick skin on opposite sides of the models. The models, designated as cones 1 and 2 in Ref. 26, are nearly identical except for the thermocouple installation techniques. The model used in this investigation is cone 2. All construction details and the method of transition detection from measured recovery temperatures are discussed in Refs. 18 and 26. The cone tips were maintained as sharp as possible to a radius of less than 0.0025 cm.

The flat-plate model is 45.7 cm long by 17.5 cm wide and is the same model used by Johnson and Kaufman[29] for heat-transfer tests in the Mach 6 High Reynolds Number Tunnel at NASA Langley. The leading edge has a bevel angle of 15 deg and thicknesses that were varied from $\bar{b} \approx 0.0025$ to 0.023 mm. Thermocouples were installed on a thin-skin 1.9 cm wide strip in the center of the model. However, heat conduction to the adjacent support structure rendered the measurement of recovery temperatures unreliable. Therefore, a surface pitot tube was used to detect transition. Morrisette and Creel[30] have verified that the surface pitot pressure and recovery temperature techniques give similar onset and end-of-transition locations on cones in this tunnel over the range of test conditions. At $M_\infty = 3.5$ and zero angle of attack, the maximum interference-free test length along the center of this plate is only 29.3 cm because of its relatively small width of 17.5 cm. Therefore, the surface pitot tube tip was set at $s_p \leq 27.9$ cm from the leading edge. Detail dimensions of the probe tip are given in the inset of Fig. 5 below.

Transition on the Sharp Cone

As discussed above, the noise incident upon the cone boundary layer was varied by operating the pilot tunnel with the bleed valve open or closed and with the cone tip set at $X_s = 12.7$ or 20.3 cm from the nozzle throat. The cone axis was aligned with the nozzle centerline. Figure 3 shows typical variations of the recovery factor r plotted against the axial distance along the cone for bleed valve open and for the cone tip located at $X_s = 12.7$ cm from the nozzle throat. Note that staggered scales are used for the ordinate in order to display the data from a single run obtained over the range of Re. The dashed lines are drawn at the theoretical laminar factor of $r_L = \sqrt{Pr} \approx 0.843$. The solid lines are for the turbulent recovery factor taken as $r_{Tu} = (Pr)^{1/3} \approx 0.892$. The onset of transition was determined as the intersection of two straight lines faired through the laminar and transitional data, as indicated in the

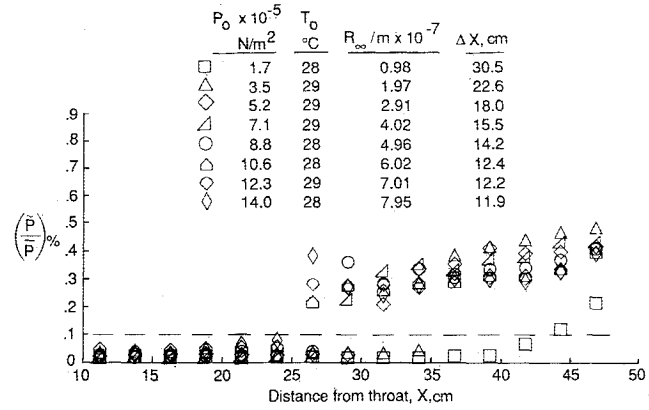

a) Bleed valve open

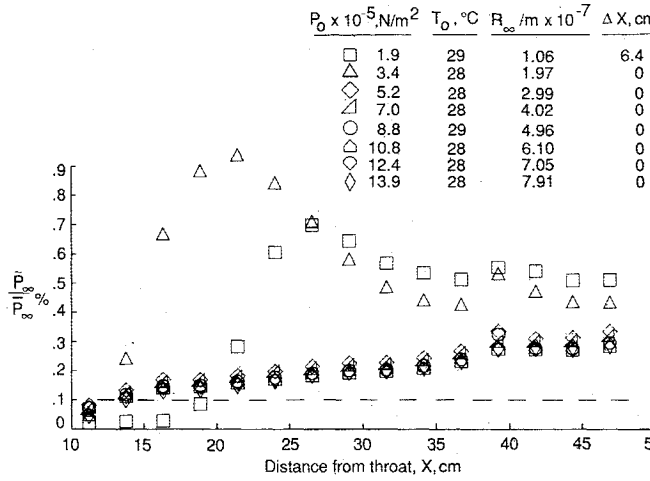

b) Bleed valve closed

Fig. 2 Variations with X of rms pressure normalized by mean static pressure along nozzle centerline.

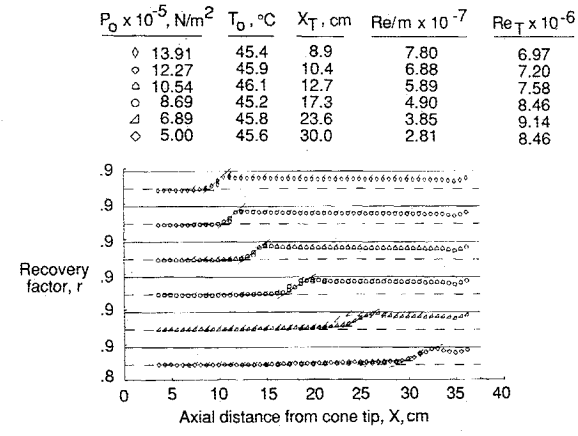

Fig. 3 Typical variations of measured recovery factor along the cone with $X_s = 12.7$ cm, main thermocouple row at top side and bleed valve open (flagged symbols are for data on the bottom side).

figure. The flagged symbols indicate data obtained from the thermocouple row on the opposite side of the main row.

All of the present transition data were determined from the main thermocouple row. Local Reynolds numbers at transition onset Re_T are plotted vs local unit Reynolds number Re in Fig. 4. For comparison, two shaded bands representing flight and conventional wind-tunnel data also are shown in Fig. 4 (sources of these flight and conventional wind-tunnel data are given in Ref. 18). The present data, with the bleed valve open, are higher than conventional wind-tunnel data by a factor of about 3. For values of $Re/m < 4\times10^7$, with the bleed valve open and the cone tip at $X_s = 12.7$ cm from the throat, some of the present data are in the range of atmospheric flight data. When the bleed valve is closed, the present data are comparable to conventional wind-tunnel data. The high transition Reynolds numbers of the present data, with the bleed valve open, are attributed to the low noise that is incident on the sensitive upstream regions of the cone boundary layer within the quiet test core. Analysis and correlation of previous results[18,31] indicated that the cone boundary layer is much more sensitive to wind-tunnel noise in the vicinity of the neutral stability point than farther downstream. Thus, when the cone is moved downstream, lower transition Reynolds numbers are generally measured because the onset of the incident noise moves upstream on the cone toward the location of the lower branch of the neutral stability curve. This situation is shown in Fig. 4 by comparison of the data with the cone tip located at $X_s = 12.7$ and 20.3 cm from the throat for the bleed valve open. The low transition Reynolds numbers for conventional wind-tunnel data and the present data with the bleed valve closed are caused by the high wind-tunnel noise incident on the entire boundary layer.

Transition on the Flat Plate

The flat plate has been tested in the pilot tunnel under run conditions similar to those with the cone. The plate surface was aligned in the ΔX and ΔZ directions (see Fig. 1) with its centerline coinciding with the nozzle centerline. The surface pitot tube, which has a height of about 0.25 mm (see inset in Fig. 5), was located in the center of the plate at a fixed distance from the leading edge. The tunnel stagnation pressure then was gradually increased to about 1.4×10^6 N/m^2, which is close to the upper limit imposed by existing valves and pipe sizes. To verify the general trends, the stagnation pressure was then reduced gradually until the supersonic flow broke down. Figure 5 shows typical values of the measured surface pitot pressures normalized by the stagnation pressure P_t/P_0 plotted against the unit Reynolds number, with the tip of the pitot tube at 27.9 cm from the leading edge. In the figure, the decreasing trends in P_t/P_0 with increasing Re are caused by the decrease in boundary-layer thickness and the corresponding increases in average Mach number over the tube height. The point just before the abrupt increase in P_t/P_0 (indicating a change to a transitional or turbulent profile) is taken as transition onset.

All flat-plate transition onset data under different conditions are plotted in Figs. 6 and 7. Because of the heat conduction problem, the wall temperature generally decreased during the run when the stagnation temperature was held nearly constant. For reference, the ratios of the mean wall temperature to the adiabatic wall temperature $\bar{T}_w/T_{aw}$ (in terms of absolute temperatures) are included in the figures. Three different thicknesses of the plate leading edge were tested. The thickness $\bar{b}$ is the nominal mean leading-edge bluntness as determined with a 70 power microscope. A sketch of the plate leading-edge geometry is shown on the inset of Fig. 7.

The flat-plate transition onset data, with $\bar{b} = 0.0025$ mm, are plotted in Fig. 6. Two 45 deg faired lines indicate data obtained by the pitot tube at two different locations of 20.3 and 27.9 cm from the plate leading edge. For the higher unit Reynolds number, the wall temperature ratios are lower because longer run times were used during the standard wind-

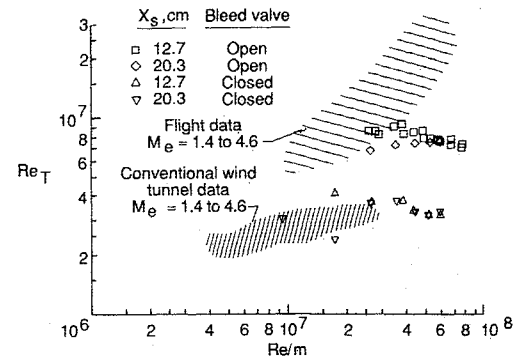

Fig. 4 Comparison of transition onset Reynolds numbers for sharp cones at zero angle of attack.

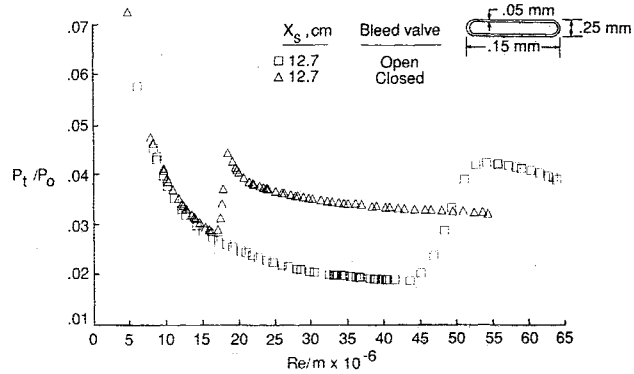

Fig. 5 Normalized surface pitot pressure as a function of local unit Reynolds number showing transition on the flat plate with the probe tip at 27.9 cm from leading edge (inset shows probe tip details).

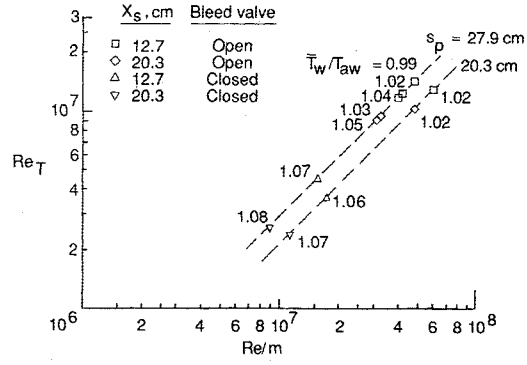

Fig. 6 Transition onset Reynolds number data on flat plate with leading-edge bluntness $\bar{b} = 0.0025$ mm (dashed lines indicate data for same probe tip location).

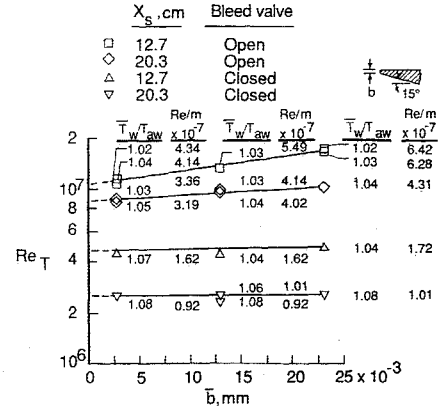

Fig. 7 Variations of transition onset Reynolds number with leading-edge bluntness (inset shows leading-edge geometry).

tunnel operating procedures. Usually, under similar tunnel conditions, the supersonic data with a lower wall temperature ratio has a higher transition Reynolds number. When the wind-tunnel noise incident on the plate is increased by either moving the plate downstream or closing the bleed valve, the transition Reynolds number is decreased. When the pitot tube location s_p is changed from 27.9 to 20.3 cm, the unit Reynolds number is increased to only a slightly higher value in order to observe transition. With this slight increase of unit Reynolds number, there are only small changes in the wind-tunnel noise conditions and hence the transition Reynolds numbers are not much different.

Figure 7 shows the effects of the plate leading-edge bluntness on the transition onset Reynolds numbers. In addition to the wall temperature ratios, the unit Reynolds numbers are also indicated for each data point in the plot. Data from similar run conditions are connected by solid lines and extrapolated to zero leading-edge thickness by dashed lines. The upper solid lines, for higher unit Reynolds numbers and lower noise conditions, show steeper slopes when compared to the lower solid lines. That is, the bluntness effects are more prominent for conditions of low noise and high unit Reynolds number. Pate's data[6] also indicated an increase of transition Reynolds numbers with increased leading-edge bluntness and increasing values of unit Reynolds number. Obviously, before the extreme sensitivity of transition to these parameters can be understood, a detailed analysis of the boundary-layer stability is required, including the effects of leading-edge thickness, the swallowing distance of the high entropy layer by the growing boundary layer, and the boundary-layer receptivity to external disturbances.

Comparisons of Cone and Flat-Plate Transition

The cone and flat-plate transition (with $\bar{b}=0.0025$ mm) onset data from Figs. 4 and 6, under the optimum low-disturbance conditions of the pilot tunnel (i.e., $X_s=12.7$ cm with the bleed valve open), are plotted in Fig. 8. Faired lines representing flat-plate data from Arnold Engineering Development Center tunnels[5] A and D and from the Jet Propulsion Laboratory 20 in. tunnel[1,32] are included for comparison. These data have all been corrected to the onset of transition and for sharp leading edges according to the best available results given in the references. The flat-plate transition Reynolds numbers from the Low-Disturbance Pilot Tunnel are about an order of magnitude higher than in the other tunnels. Also, comparison of the present cone and flat-plate data shows that the cone data are considerably lower than the flat-plate data. These data are in excellent agreement with the predictions of the e^N method ($N=10$) using compressible linear stability theory. The theoretical predictions will be discussed in the next section.

Figure 9 is taken from Pate's correlation for the ratios of cone-to-flat-plate transition Reynolds numbers.[4,6] The upper shaded band represents Pate's results for the end of transition from five different wind tunnels. The present results for the onset of transition at $M_\infty=3.5$ from Figs. 4 and 7 (with $\bar{b}$ extrapolated to 0) are included for comparison. Although the onset of transition is better suited for comparison with stability theory, since the length of the transition region varies considerably in different tunnels and has already been shown to depend on noise intensities (see Fig. 9 and Ref. 31), the ratios of cone-to-flat-plate transition Reynolds numbers obtained from the present data are not much different for transition onset or transition end. Therefore, Pate's data are not corrected to transition onset in this figure. Since the present cone data are for $T_w=T_{aw}$ and the flat-plate data are for $T_w>T_{aw}$, ratios of the cone-to-flat-plate transition Reynolds numbers would have been somewhat lower than those shown in Fig. 9 if $T_w=T_{aw}$ during the test on the plate. To illustrate the effects of slight changes in T_w/T_{aw} on these ratios, predictions of the e^N method with $N=10$ are shown in Table 1. A discussion of the theoretical predictions is presented in the next section. No

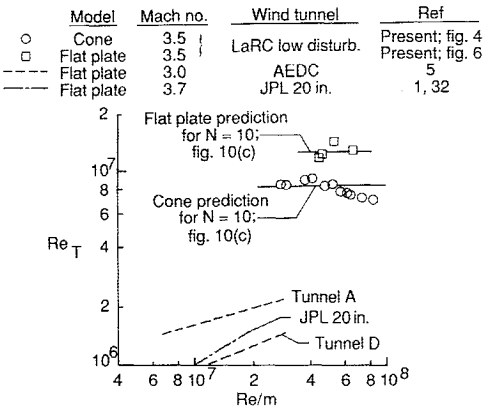

Fig. 8 Comparison of transition onset Reynolds numbers on cone and flat plate with $\bar{b}=0.0025$ mm.

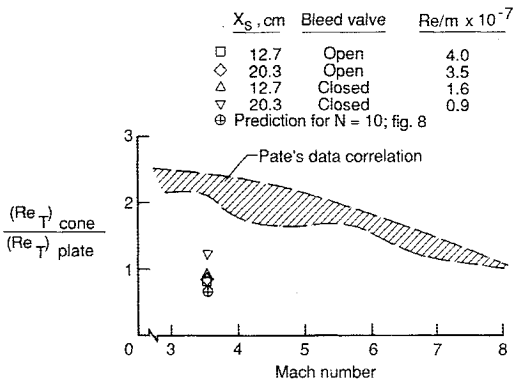

Fig. 9 Ratios of cone-to-flat-plate transition Reynolds numbers from Pate[4,6] compared with the present data and the prediction from linear stability theory.

Table 1 Predictions of e^N method ($N=10$)

T_w/T_{aw}	Re_T with $N=10$	$Re_{T_{cone}}/Re_{T_{plate}}$
On sharp leading-edge flat plate		
1.00	12.3×10^6	0.68
1.03	11.9×10^6	0.70
1.07	10.8×10^6	0.77
On sharp tip 5 deg half-angle cone		
1.00	8.34×10^6	

corrections of the present flat-plate data to adiabatic wall conditions have been attempted in this report.

Depending on nozzle noise conditions, the present data for $M_\infty=3.5$ show the ratios of cone-to-flat-plate transition Reynolds numbers varied from about 0.8 up to about 1.2, which are much less than Pate's data. The prediction for $M_\infty=3.5$ and $N=10$, for adiabatic wall conditions, is very close to the present data under the optimum low-disturbance conditions of the pilot tunnel. The reason for these results is that, under the optimum low-disturbance conditions, the acoustic energy radiated to the upstream sensitive regions of the cone and flat-plate boundary layers is extremely small at all frequencies. The higher ratios of cone-to-flat-plate transition Reynolds numbers of the present data under higher noise conditions may be due to faster growth of the boundary-layer thickness on the flat plate than on the cone and, thus, stronger receptivity of the flat-plate boundary layer to the incident acoustic field. The even higher ratios of Pate's data are caused by the facts that the most amplified frequencies on the flat plate are lower than those on the cone (see next section) and that the thick turbulent boundary layers on the nozzle walls of

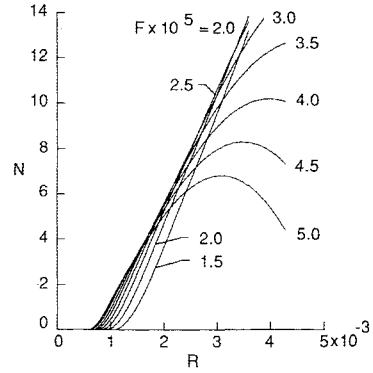

a) Cone

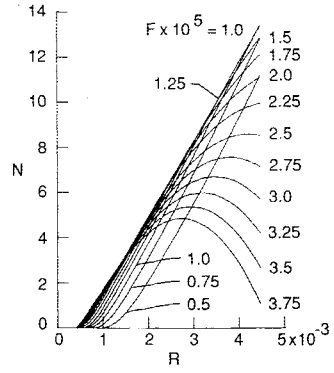

b) Flat plate

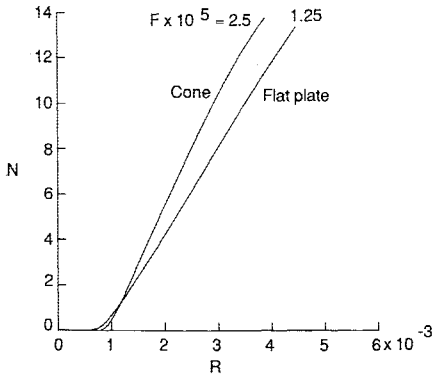

c) Comparison of cone and flat plate for the most amplified frequencies at $N = 10$

Fig. 10 N-factor envelope curves at $M_\infty = 3.5$.

conventional wind tunnels radiate more acoustic energy at low frequencies than at high frequencies. These results emphasize dramatically the importance of using quiet tunnels for high-speed transition studies.

Transition Predictions for a Cone and Flat Plate at $M_\infty = 3.5$

Compressible three-dimensional linear stability equations with the assumptions of parallel flow and variable Prandtl number were solved (using a modified version of the COSAL code[33]) to obtain the disturbance amplification rate $\sigma(s)$ needed for computation of the N factor, which is defined as

$$N = \int_{s_0}^{s} \sigma(s)\, ds$$

where s is the distance along the cone or flat plate from the tip or the leading edge and s_0 the location of the onset of instability. Calculations were made for various disturbance frequencies and the N factor curves for the adiabatic wall cone and flat plate are plotted separately in Figs. 10a and 10b. Figure 10c shows the variation of N and R for only those frequencies that first reached the value $N = 10$. At this value of N, the predicted transition of Reynolds numbers for a cone and flat plate are in excellent agreement with the observed transition Reynolds numbers (Figs. 8 and 9). Malik[15] previously made complete stability calculations for cones applicable to flight data and selected data from the Mach 3.5 Pilot Low-Disturbance Tunnel. The values of N computed at the measured onset locations of transition varied about 9–11. Thus, it is concluded that similar values of N are also applicable to the flat-plate data when the tunnel disturbances incident upon the upstream sensitive regions of the boundary layer are small.

Figure 10c shows that the most amplified dimensionless frequencies for the cone and flat plate for $N = 10$ are $F \times 10^5 = 2.5$ and 1.25, respectively (where $F = 2\pi f \nu_e / u_e^2$). The higher frequencies for the cone are due to the smaller boundary-layer thickness on the cone. Hence, for amplification to $N = 10$, the flat-plate boundary layer is more sensitive to low frequencies than the cone boundary layer. Figures 10a and 10b also show the same relative sensitivities to frequencies for small values of R near the neutral stability region. These results could account for the lower transition Reynolds numbers usually measured on flat plates than on cones in conventional tunnels where the thick turbulent boundary layers on the nozzle walls radiate more energy at low frequencies than at high frequencies.

Conclusions

1) Transition Reynolds numbers on a flat plate under low-noise conditions in the Mach 3.5 Pilot Low-Disturbance Tunnel are nearly an order of magnitude higher than from previous investigations in conventional noisy tunnels.

2) The ratios of cone-to-flat-plate transition Reynolds numbers vary from about 0.8 under low-noise conditions up to 1.2 under high-noise conditions in the Mach 3.5 Pilot Low-Disturbance Tunnel, as compared to values of about 2.2–2.5 for this ratio in conventional noisy tunnels. This result implies that flat-plate boundary layers are much more receptive to wind-tunnel noise than cone boundary layers.

3) The stability calculations indicate that, for low-noise conditions, the most amplified frequencies leading to transition are considerably higher on the cone than the flat plate.

4) Calculations based on compressible linear stability theory in conjunction with the e^N method are in excellent agreement with transition data on both the cone and flat plate for $N = 10$ when the upstream regions of the models are in the quiet flow test region. The present results under low-disturbance condition therefore have resolved the discrepancies that have existed between linear stability theory results and transition data from conventional supersonic wind tunnels.

Summarizing the above conclusions, this investigation demonstrates that transition results obtained in conventional noisy wind tunnels generally do not simulate flight conditions correctly, including the relative locations of transition on two-dimensional and axisymmetric configurations.

References

[1]Laufer, J. and Marte, J. E., "Results and a Critical Discussion of Transition-Reynolds-Number Measurements on Insulated Cones and Flat Plates in Supersonic Wind Tunnels," Jet Propulsion Laboratory, Pasadena, CA, JPL Rept. 20-96, 1955.

[2]Potter, J. L. and Whitfield, J. D., "Boundary-Layer Transition under Hypersonic Conditions," *AGARDograph* 97, Pt. III, 1965.

[3]Mack, L. M., "Recent Developments in Boundary Layer Transition Research," *AIAA Journal*, Vol. 3, March 1975, pp. 278–289.

[4]Pate, S. R., "Measurements and Correlations of Transition Reynolds Numbers on Sharp Slender Cones at High Speeds," Arnold Engineering Development Center, Arnold AFB, TN, AEDC-TR-69-172, 1969 (also *AIAA Journal*, Vol. 9, June 1971, pp. 1082–1090).

[5]Pate, S. R. and Scheuler, C. J., "Radiated Aerodynamic Noise Effects on Boundary-Layer Transition in Supersonic and Hypersonic Wind Tunnels," *AIAA Journal*, Vol. 7, March 1969, pp. 450–457.

[6]Pate, S. R., "Dominance of Radiated Aerodynamic Noise of Boundary-Layer Transition in Supersonic-Hypersonic Wind Tunnels—Theory and Application," Arnold Engineering Development Center, Arnold AFB, TN, AEDC-TR-77-107, 1978.

[7]Strike, W. T., Jr., Donaldson, J. C., and Beale, D. K., "Test Section Turbulence in the AEDC/VKF Supersonic/Hypersonic Wind Tunnels," Arnold Engineering Development Center, Arnold AFB, TN, AEDC-TR-81-5, 1981.

[8]Mack, L. M., "Boundary-Layer Stability Analysis for Sharp Cones at Zero Angle of Attack," Air Force Wright Aeronautical Lab., Wright-Patterson AFB, OH, AFWAL-TR-86-3022, Aug. 1986.

[9]Malik, M. R., "Prediction and Control of Transition in Hypersonic Boundary Layers," AIAA Paper 87-1414, June 1987.

[10]Smith, A. M. O., "On the Growth of Taylor-Görtler Vortices along Highly Concave Walls," *Quarterly Applied Mechanics*, Vol. XIII, No. 3, Oct. 1955, pp. 233–262.

[11]Jaffe, N. A., Okamura, T. T., and Smith, A. M. O., "Determination of Spatial Amplification Factors and Their Application to Predicting Transition," *AIAA Journal*, Vol. 8, Feb. 1970, pp. 301–308.

[12]Merkle, C. L., Ko, D. R. S., and Kubota, T., "The Effect of Axisymmetric Geometry on Boundary-Layer Transition as Predicted by Linear Stability Theory," Flow Research, Inc., Washington, DC, Rept. 39, Sept. 1974.

[13]Wazzan, A. R., Gazley, C., Jr., and Smith, A. M. O., "Tollmien-Schlichting Waves and Transition," *Progress in Aerospace Sciences*, Vol. 18, 1979, pp. 351–392.

[14]Malik, M. R., Wilkinson, S. P., and Orszag, S. A., "Instability and Transition in Rotating Disk Flow," *AIAA Journal*, Vol. 19, Sept. 1981, pp. 1131–1138.

[15]Malik, M. R., "Instability and Transition in Supersonic Boundary Layers. Laminar-Turbulent Boundary Layers," *Proceedings of Energy Resources Technology Conference*, edited by E. M. Uram and H. E. Weber, American Society of Mechanical Engineers, New York, Feb. 1984, pp. 139–147.

[16]Beckwith, I. E., Malik, M. R., Chen, F.-J., "Nozzle Optimization Study for Quiet Supersonic Wind Tunnels," AIAA Paper 84-1628, June 1984.

[17]Malik, M. R. and Poll, D. I. A., "Effect of Curvature on Three-Dimensional Boundary-Layer Stability," *AIAA Journal*, Vol. 23, Sept. 1985, pp. 1362–1369.

[18]Beckwith, I. E., Creel, T. R., Jr., Chen, F.-J., and Kendall, J. M., "Free-Stream Noise and Transition Measurements on a Cone in a Mach 3.5 Pilot Quiet Tunnel," NASA TP-2180, Sept. 1983.

[19]Beckwith, I. E., Chen, F.-J., and Creel, T. R., Jr., "Design Requirements for the NASA Langley Supersonic Low-Disturbance Wind Tunnel," AIAA Paper 86-0763, March 1986.

[20]Brinich, P. F., "Effects of Bluntness on Boundary Layer Transition at Mach 3.1," NACA TN 3659, March 1956.

[21]Moeckel, W. E., "Some Effects of Bluntness on Boundary Layer Transition and Heat Transfer at Supersonic Speeds," NACA Rept. 1312, Oct. 1957.

[22]Reshotko, E. and Khan, M. M. S., "Stability of the Laminar Boundary Layer on a Blunted Plate in Supersonic Flow," *Proceedings of IUTAM Laminar-Turbulent Transition Symposium*, Springer-Verlag, Berlin, FRG, Sept. 1979, pp. 186–200.

[23]Jillie, D. W. and Hopkins, E. J., "Effects of Mach Number, Leading-Edge Bluntness, and Sweep on Boundary Layer Transition on a Flat Plate," NASA TN D-1071, Sept. 1961.

[24]Stetson, K. F. and Rushton, G. H., "Shock Tunnel Investigation of Boundary Layer Transition at $M=5.5$," *AIAA Journal*, Vol. 5, May 1967, pp. 899–906.

[25]Stetson, K. F., "Effect of Bluntness and Angle of Attack on Boundary Layer Transition on Cones and Biconic Configurations," AIAA Paper 79-0269, Jan. 1979.

[26]Creel, T. R., Jr., Beckwith, I. E., and Chen, F.-J., "Nozzle Wall Roughness Effects on Free-Stream Noise and Transition in the Pilot Low-Disturbance Tunnel," NASA TM-86389, Sept. 1985.

[27]Beckwith, I. E., "Comments on Settling Chamber Design for Quiet, Blowdown Wind Tunnels," NASA TM-81948, March 1981.

[28]Beckwith, I. E., Chen, F.-J., and Malik, M. R., "Design and Fabrication Requirements for Low-Noise Supersonic/Hypersonic Wind Tunnels," AIAA Paper 88-0143, Jan. 1988.

[29]Johnson, C. B. and Kaufman, L. G., II, "Interference Heating from Interactions of Shock Waves with Turbulent Boundary Layers at Mach 6," NASA TN D-7649, Sept. 1974.

[30]Morrisette, E. L. and Creel, T. R., Jr., "The Effects of Wall Surface Defects on Boundary-Layer Transition in Quiet and Noisy Supersonic Flow," NASA CP 2487, Pt. 3, March 1987, pp. 965–980.

[31]Chen, F.-J., Beckwith, I. E., and Creel, T. R., Jr., "Correlations of Supersonic Boundary-Layer Transition on Cones Including Effects of Large Axial Variations in Wind-Tunnel Noise," NASA TP-2229, Jan. 1984.

[32]Coles, D., "Measurements of Turbulent Friction on a Smooth Flat Plate in Supersonic Flow," *Journal of the Aeronautical Sciences*, Vol. 21, July 1954, pp. 433–448.

[33]Malik, M. R., "COSAL—A Black-Box Compressible Stability Analysis Code for Transition Prediction in Three-Dimensional Boundary Layers," NASA CR-165925, May 1982.